Polymer Degradation and Stability 97 (2012) 1297–1304

Contents lists available at SciVerse ScienceDirect

Polymer Degradation and Stability

journal homepage: www.elsevier.com/locate/polydegstab

Thermal stability of polycarbonate-graphene nanocomposite foams

G. Gedler, M. Antunes, V. Realinho, J.I. Velasco*

Centre Català del Plàstic, Departament de Ciència dels Materials i Enginyeria Metal·lúrgica, Universitat Politècnica de Catalunya, BarcelonaTech. C/Colom 114, E-08222 Terrassa (Barcelona), Spain

ARTICLE INFO

Article history:
Received 17 May 2012
Accepted 22 May 2012
Available online 29 May 2012

Keywords:
Polycarbonate
Graphene
Foams
Thermal stability

ABSTRACT

A thermogravimetric study in both nitrogen and air atmospheres has been carried out on unfilled and graphene-reinforced solid and foamed polycarbonate. Polycarbonate foams were prepared using a supercritical CO_2 dissolution one-step batch foaming process. Results showed that polycarbonate displayed a characteristic one-step decomposition under nitrogen, while three-step degradation was observed in air. In addition, as-received pristine graphene nanoplatelets displayed a three-step degradation in air, compared to a mild degradation under nitrogen. It was found that the thermal stability remarkably improved for the foamed composites, related to a combination of a heat transfer reduction promoted by the insulating cellular structure and the presence of the platelet-like graphene, which helped create a physical barrier effect, delaying the escape of volatile products generated during decomposition.

1. Introduction

Graphene-based polymer composites have been the subject of interest in recent years, mainly due to the combination of high thermal, mechanical and electrical properties of graphene, a monolayer of sp^2-hybridized carbon atoms arranged in a two-dimensional lattice [1]. Its incorporation into polymers may result in remarkable improvements of the host material [2–4]. The outstanding thermal stability of graphene makes it a very attractive material for the fabrication of polymer composites with improved thermal stabilities. Particularly, the thermal degradation of polymers such as PVA [5,6], PMMA [7], PS [8], polyaniline [9] or PP [10] using different types of graphene have been studied in the last few years, with important improvements in thermal stability being found for these composites. Another characteristic of graphene that could have an important effect in the thermal degradation is its particular flat-like morphology, which, depending on the dispersion and exfoliation degree of graphene nanoplatelets within the matrix, could promote a physical barrier effect to volatile gases generated during decomposition [11]. Hence, the dispersion of graphene in the polymer could have an important effect in the composites' decomposition mechanism. Several different techniques have been carried out in order to improve the dispersion of nano-sized fillers in composites. In situ polymerization [12,13], solution blending [14–17], or the combination of different melt-mixing techniques [13] have been used. However, these techniques limit the amount of produced composite. Currently, the trend is looking for mechanical, thermal and electrical improvements in composites with the smallest amounts of graphene using conventional industrial processing techniques such as extrusion.

Owing to its high mechanical properties and thermal stability, polycarbonate (PC) is one of the most used engineering plastics. Detailed investigations of the thermal degradation of PC have been successfully carried out. For instance, thermogravimetric analyses have been carried out in order to study the thermal behaviour of PC [18–22]. The thermal degradation pathways of PC in different atmospheres have been widely discussed [21,22]. Though studies of the thermal stability of PC composites with a silicate-layered nanoclay, montmorillonite, have been carried out [23,24], information regarding PC-graphene composites is still lacking.

The increasing interest in multifunctional materials and structures is driven by the need for the development of new materials that may combine structural functions with more functional characteristics, such as improved transport properties [25]. One possible strategy considers foaming of the base material and the control of its final cellular structure [26]. However, knowledge of the thermal stability of foams made from PC-graphene is still pretty scarce, mainly due to their multiphase complex nature. So far, only a few works have investigated the thermal degradation of graphene-based foamed composites, using silicone [27] and polystyrene [28] as polymer matrices.

In the present study, we conducted a thermogravimetric analysis on unfilled and graphene-reinforced solid and foamed

* Corresponding author. Tel.: +34 937837022; fax: +34 937841827.
E-mail address: jose.ignacio.velasco@upc.edu (J.I. Velasco).

0141-3910/$ – see front matter © 2012 Elsevier Ltd. All rights reserved.
doi:10.1016/j.polymdegradstab.2012.05.027

polycarbonate composites that helped us to understand the effects of incorporating graphene nanoplatelets and foaming, as well as a combination of both, on the thermal stability of the prepared foams.

2. Experimental

2.1. Materials preparation

Composite preparation consisted in melt-compounding a pelletized polycarbonate (Lexan-123R-PC, supplied by Sabic, with a density of 1.2 g/cm^3 and MFI of 17.5 dg/min, measured at 300 °C and 1.2 kg) with 0.5 wt% of graphene nanoplatelets using a Brabender Plasticorder internal mixer at a constant temperature of 180 °C and screw speeds of 30, 60 and 120 rpm during a mixing time of 1, 2 and 3 min respectively.

The graphene nanoplatelets used in this study, with the commercial name of xGnP-M-15, so-called for now on GnP, were supplied by XG Sciences, Inc. These graphene nanoplatelets are 6–8 nm thick with a 15 μm average diameter, a typical surface area of 120–150 m^2/g and a density of 2.2 g/cm^3, as reported by the manufacturer.

After removing from the mixer, the graphene-reinforced PC composite was placed in a 3.5 mm-thick circular mould and compression-moulded at 220 °C and 45 bar using a hot-plate press *IQAP-LAP PL-15*. Once cooled under pressure at 45 bar using a water cooling system, the solid discs were removed from the mould and used as foaming precursors. These solid foaming precursors were later saturated with CO_2 and foamed using a one-step batch foaming process according to the procedure explained in one of our previous works [29].

2.2. Testing procedure

Thermogravimetric analysis was performed in a TGA/DSC 1 Mettler Toledo Star System analyser by heating samples of around 10.0 mg from 30 to 1000 °C at a heating rate of 10 °C/min under both nitrogen (constant 30 ml/min N_2 flow) and air atmospheres (constant 60 ml/min air flow). The temperatures corresponding to mass losses of 1, 5 and 50%, as well as the mass of the final residue obtained at 1000 °C, were reported for the unfoamed and foamed unfilled and graphene-reinforced polycarbonate composites.

X-ray diffraction (XRD) was carried out using a Panalytical diffractometer operating with CuKα radiation ($\lambda = 0.154$ nm) at 40 kV and 40 mA. Scans were taken from 2 to 60° with a scan step size of 0.02°.

In order to observe the stacks of graphene platelets distributed within the cell struts of the foamed composites and have an idea of their main dimensions, a JEOL JSM-5610 scanning electron microscope was used, with a voltage of 15 kV and a working distance of 30 mm. Samples were previously prepared by fracturing at room temperature and depositing a thin layer of gold at their surface using a BAL-TEC SCD005 Sputter Coater in argon atmosphere.

3. Results and discussion

3.1. Thermogravimetric analysis

The TGA and respective DTG thermograms of the solid and foamed unfilled polycarbonate (respectively called PC and PC-f), as well as the solid and foamed graphene-reinforced composites (respectively, PCg and PCg-f), were obtained under both nitrogen and air atmospheres. A characteristic one-step decomposition was observed under nitrogen atmosphere, while three-step degradation was observed in air. Additional thermogravimetric analysis was carried out under both atmospheres on the original powder-like graphene nanoplatelets. The results are depicted in Tables 1 and 2 and discussed as follows.

3.1.1. Thermogravimetric analysis under nitrogen atmosphere

3.1.1.1. Unfilled polycarbonate. The TGA and respective DTG thermograms of the unfilled solid polycarbonate (PC), presented in Fig. 1a, showed a characteristic one-step decomposition with an onset temperature at 1 wt% loss of 388 °C and a T_{max}, defined as the temperature at maximum mass loss rate in the DTG curve, of 430 °C. It is well known that the main degradation pathways of polycarbonate can be classified into two categories [21]: chain scission of isopropylidene bonds and hydrolysis/alcoholysis of carbonate bonds, including rearrangements of some carbonate bonds like decarboxylation or cross-linking upon heating, ultimately resulting in CO_2, H_2O and char.

The corresponding DTG thermogram suggested that two events could be occurring at a different rate due to the shoulder observed in Fig. 1a, related on one side to a smaller quantity of material undergoing the degradation at that temperature, and on the other to the two peaks observed in the heat flow curve (Fig. 1b), indicating that two different exothermic processes were taking place. The first peak was attributed to the chain scission of isopropylidene bonds (stage I), starting the degradation in accordance with the bond dissociation energies [21], while the second one was related to the hydrolysis and alcoholysis of carbonate bonds as well as the rearrangements of some carbonate bonds with continuing the chain scission (stage II). A wider and also intense peak was observed during this second process, related to a more exothermic decomposition. After this decomposition, there was a temperature range where the process slowed down due to the amount of material remaining.

Though the unfilled foamed polycarbonate (PC-f) showed a similar one-step decomposition, there was a delay corresponding to the beginning of the process for a 1 wt% loss of about 34 °C and of 55 °C for a 5 wt% loss when compared to the solid material. The DTG curve showed how the degradation occurred faster than for the solid PC, though with a T_{max} about 70 °C higher (see Fig. 1a). The delay during the beginning of the degradation was attributed to the material's cellular structure, which acted as an improved thermal insulator, inhibiting heat transfer at the beginning of the thermal decomposition. The high mass loss rate can be explained as follows: the cellular structure of the material is filled with air, as well as some remaining CO_2 from the foaming. As a result of the presence of the aforementioned gases, in addition to the start of the external degradation of the material, a simultaneous internal degradation

Table 1
TGA and DTG data under nitrogen atmosphere obtained at 10 °C/min.

Material code	Temperature (°C)				Residue at 1000 °C (wt%)	Relative density
	1 wt% loss	5 wt% loss	50 wt% loss	Max. mass loss rate		
PC	388	407	465	430	16	1.00
PC-f	422	449	500	500	20	0.43
	421	452	512	512	23	0.38
	417	451	510	510	22	0.46
	420	442	497	497	21	0.46
PCg	422	462	503	493	21	1.00
PCg-f	450	477	517	515	24	0.49
	431	462	513	512	23	0.47
	444	474	516	515	22	0.79
	436	467	510	507	22	0.59
	436	469	515	513	23	0.38
	461	484	519	517	25	0.35

Table 2
TGA and DTG data under air atmosphere obtained at 10 °C/min.

Material code	Temperature (°C)						Residue at 1000 °C (wt%)	Relative density
	1 wt% loss	5 wt% loss	50 wt% loss	T_{max1} [a]	T_{max2} [b]	T_{max3} [c]		
PC	356	406	488	451	496	594	0	1.00
PC-f	377	420	479	475	492	610	0	0.43
	377	414	476	467	492	610	0	0.38
	381	428	505	506	517	616	0	0.46
	395	434	492	485	503	609	0	0.46
PCg	386	423	504	498	515	609	0.66	1.00
PCg-f	379	422	488	479	499	610	0.76	0.49
	398	431	493	485	501	614	0.60	0.47
	380	412	477	472	500	609	0.14	0.79
	404	442	509	508	513	611	0.25	0.59
	391	434	504	503	508	610	0.40	0.38
	394	443	506	501	517	625	0	0.35

[a] Temperature at maximum rate of mass loss corresponding to step I.
[b] Temperature at maximum rate of mass loss corresponding to step II.
[c] Temperature at maximum rate of mass loss corresponding to step III.

takes place due to the oxidative action of the small quantity of air present, resulting in an increased mass loss rate.

The heat flow curve, presented in Fig. 1b, clearly showed two smaller peaks compared to the neat PC due to the presence of the cellular structure, corresponding respectively to stage I and stage II of the decomposition of polycarbonate. Once again and in a similar manner as the unfilled solid PC, the first observed exothermic peak (stage I) was related to the scission of the isopropylidene and carbonate bonds, while the second one (stage II) was due to the alcoholysis/hydrolysis.

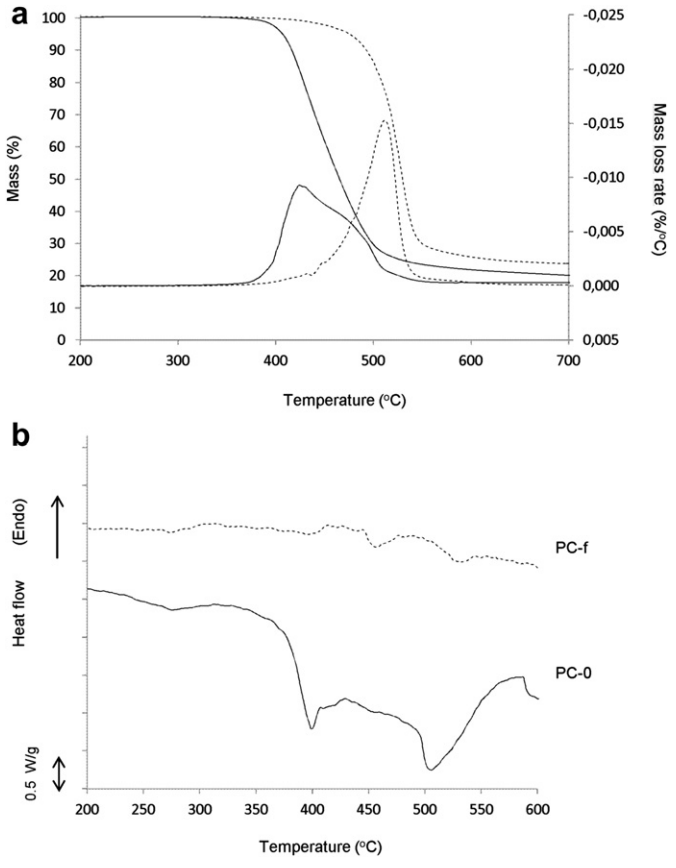

Fig. 1. (a) TGA and DTG thermograms and (b) heat flow curves under nitrogen atmosphere for the unfilled solid (PC, continuous line) and foamed polycarbonate (PC-f, relative intensity: 0.38, dashed line), obtained at a heating rate of 10 °C/min.

3.1.1.2. Graphene nanoplatelets (GnP). The TGA and DTG curves of graphene nanoplatelets in nitrogen are shown together in Fig. 2. As can be seen, graphene showed a very stable thermal behaviour, presenting a total weight loss of 10% at 1000 °C. The first weight loss stage was observed around 100 °C, related to the removal of physically adsorbed water [10]. After that, graphene exhibited a smooth two-step degradation with maximum weight losses taking place respectively at 200 and 630 °C, representing a 7% of the total weight, which were related to the removal of oxygen-containing functional groups such as ethers, carboxyls or hydroxyls [30]. These formed due to the presence of residual acid used by the manufacturer in the chemical-thermal exfoliation process of graphene synthesis [31]. The graphene nanoplatelets presented a temperature corresponding to a 1 wt% loss of 168 °C, while a temperature of 460 °C was obtained for a 5 wt% loss. Following these important weight losses, a final process at around 990 °C with a weight loss of about 5% was detected. This could be related to the degradation of the small amount of char formed during the previous degradation steps.

3.1.1.3. Graphene-reinforced polycarbonate. As can be seen in Fig. 3a, the degradation of graphene-reinforced polycarbonate composites (PCg) followed a characteristic one-step decomposition, with important decomposition delays during degradation when compared to unfilled PC. Particularly, PCg presented a 34, 55

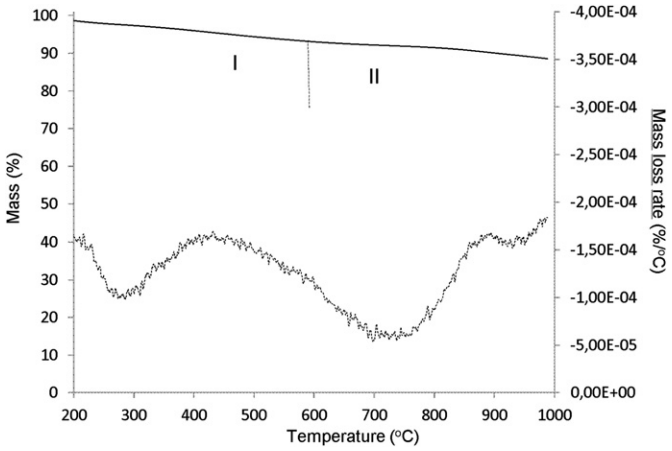

Fig. 2. TGA and DTG thermograms under nitrogen atmosphere for the original graphene nanoplatelets (GnP), obtained at a heating rate of 10 °C/min.

and 38 °C decomposition delay corresponding respectively to 1, 5 and 50 wt% losses (see Table 1). Also, the DTG curve showed how the T_{max} for PCg increased when compared to PC, which can be attributed to the presence of the graphene nanoplatelets, as it is well known that on one hand graphene presents a high thermal stability, and secondly its particular flat-like morphology may promote a gas barrier effect like other fillers with similar morphology [32]. The resulting gas tortuous path effect may be created by the well dispersed graphene nanoplatelets, delaying the escape of volatile degradation products during decomposition [33], hence globally improving the thermal stability. The analysis of the heat flow curves presented in Fig. 3b shows how the beginning of the first exothermic process was significantly delayed due to the tortuous path to gas escape formed by the graphene nanosheets, suggesting that stages I and II merged closely to only one peak, resulting in more thermally stable materials.

The graphene-reinforced foamed polycarbonate (PCg-f) followed a similar one step degradation. A slight temperature increment shift in the degradation was noticed when compared to the graphene-reinforced solid (PCg), with a temperature difference of 30 °C for a 1 wt% loss, and of 12 °C for both 5 and 50 wt% losses (see results presented in Table 1). The DTG curves presented in Fig. 4a show how the T_{max} for PCg-f shifted towards a higher value when compared to PCg, indicating that the major degradation was occurring at different times and rates. Particularly, this delay was attributed to the cellular structure of the foam, which increased the rate of mass loss, in a similar way as explained previously for the unfilled PC foams (PC-f).

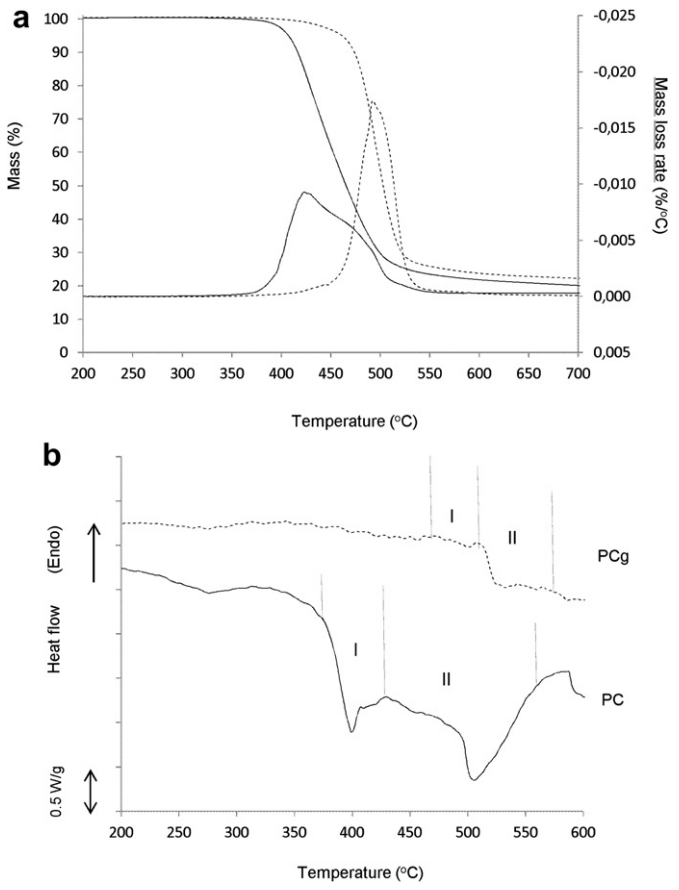

Fig. 3. (a) TGA and DTG thermograms and (b) heat flow curves under nitrogen atmosphere for the unfilled solid (PC, continuous line) and graphene-reinforced solid polycarbonate (PCg, dashed line), obtained at a heating rate of 10 °C/min.

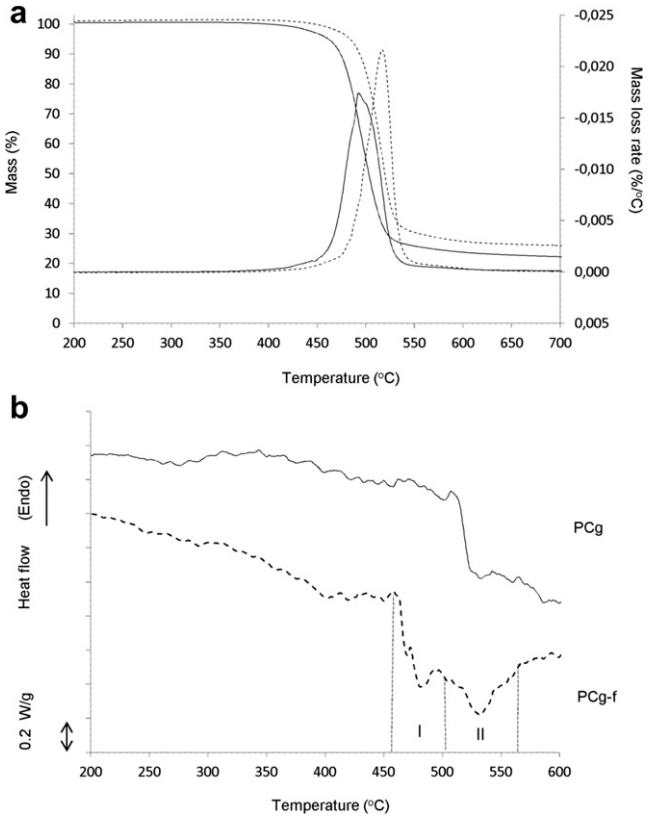

Fig. 4. (a) TGA and DTG thermograms and (b) heat flow curves under nitrogen atmosphere for the graphene-reinforced solid (PCg, continuous line) and graphene-reinforced foamed polycarbonate (PCg-f, relative density: 0.38, dashed line), obtained at a heating rate of 10 °C/min.

Similar thermal degradation processes could also be observed in terms of the heat flow curves (Fig. 4b), once again the two peaks almost merged completely as for the PCg and the decomposition temperature shifted to higher values when compared to the unfilled materials.

A comparison of the evolution of the decomposition temperature corresponding to 1, 5 and 50 wt% loss with relative density is given in Fig. 5a between the unfilled foamed polycarbonate (PC-f) and the graphene-reinforced foam (PCg-f). Interestingly, the foams with lower relative density displayed highest delays regarding the decomposition temperature, which was related to their more effective thermal insulating cellular structure. When the thermal decomposition reached higher mass loss percentages, the thermal stability mainly depended on the protective structure formed by the char product generated during the early stages of degradation, acting as a physical barrier, protecting the unburned polymer matrix from heat as well as retarding the diffusion of pyrolysis gases [23]. Generally speaking, graphene-reinforced composites with relative densities between 0.6 and 1 presented better thermal stabilities than unfilled PC, mainly related to the presence of graphene. For lower relative densities, the thermal behaviour of composites was very similar to that of unfilled PC, though the presence of graphene still provided better thermal stability. This difference was reduced with increasing mass loss. A solid char residue between 17 and 25 wt% remained at the end of the decomposition, i.e., at 1000 °C.

3.1.2. Thermogravimetric analysis under air atmosphere

3.1.2.1. Unfilled polycarbonate. The thermal decomposition of polycarbonate in air occurred in three stages, as can be seen in Fig. 6.

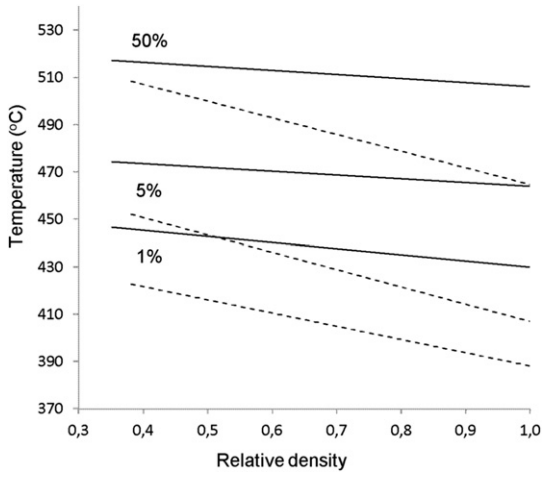

Fig. 5. Evolution of the decomposition temperature corresponding to 1, 5 and 50 wt% loss with relative density tested under nitrogen atmosphere (10 °C/min heating rate) for the unfilled (PC-f, dashed line) and graphene-reinforced foamed polycarbonate (PCg-f, continuous line).

The first stage corresponded to the thermo-oxidative decomposition of polycarbonate in air. This stage can be explained looking at the exothermic process showed in the heat flow curve presented in Fig. 6b, where A, B and C represent each of the decomposition exothermic processes involved. The degradation started with the chain scission of the isopropylidene bonds, including alcoholysis and hydrolysis of the carbonate bonds, similar to that under nitrogen atmosphere, associated to the A + B peak. The third and very sharp peak (C) suggested branching, cross linking and peroxide formation reactions, which underwent dissociation promoted by the presence of oxygen. During this stage a char layer

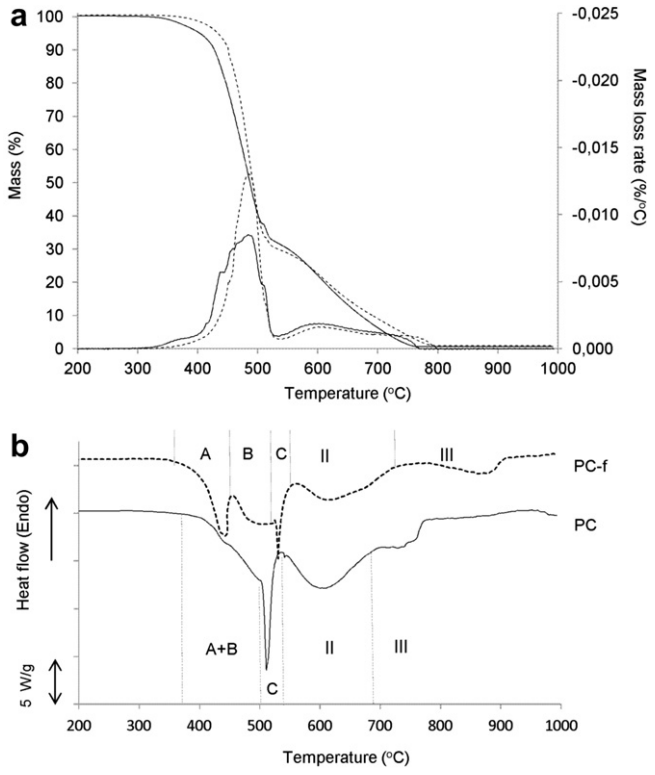

Fig. 6. (a) TGA and DTG thermograms and (b) heat flow curves under air atmosphere for the unfilled solid (PC, continuous line) and foamed polycarbonate (PC-f, relative intensity: 0.38, dashed line), obtained at a heating rate of 10 °C/min.

formed at the materials surface, inhibiting the access of air to the unburned polymer and acting as an insulating layer that slowed down degradation [23,31]. This increased the probability for radical recombination reactions in the condensed phase [22]. It is important to highlight that the peaks corresponding to the exothermic processes were much higher than those obtained under nitrogen, related to the thermo-oxidative degradation promoted by the oxygen present in air.

The second stage (stage II) of the degradation presented a slighter mass loss slope than the first main stage of degradation and had the shortest period of time of the three main degradation stages. This stage was attributed to the decomposition of the remaining polymer that was kept protected from burning due to the char layer formed during stage I, as well as the degradation of part of that previous char layer. Also shown in Fig. 6b is stage III, which was attributed to char oxidation produced in the previous stages that allowed trapped gases to escape [34]. This last stage was also clearly observed in TGA and DTG thermograms (Fig. 6a), presenting a steeper slope when compared to stage II, which was related to a faster degradation. Nevertheless, this process was still slower than the decomposition corresponding to stage I. No solid residues were obtained after 1000 °C, indicating a complete thermo-oxidative decomposition of polycarbonate.

Fig. 6a also shows the three-step degradation of the unfilled foamed polycarbonate (PC-f). There was a shift in the temperature corresponding to the first decomposition stage towards higher values when compared to the unfilled solid PC, for instance the 1 and 5 wt% loss temperatures being delayed in 25 °C and 30 °C, respectively. The DTG showed how the degradation occurred faster than for the unfilled solid PC, though with a T_{max} about 30 °C higher (see Fig. 6a). The delay observed during the beginning of the degradation was once again attributed to the cellular structure, which acted as a thermal insulator within the material, inhibiting heat transfer at the beginning of the thermal decomposition. The higher mass loss rate of PC-f when compared to PC can be explained in a similar manner as the differences explained previously under nitrogen atmosphere. The heat flow curve (Fig. 6b) displayed an exothermic decomposition (stage I) which could be separated in three different exothermic peaks: A, B and C. Peak A corresponded to the scission of the isopropylidene bonds and some carbonate bonds undergoing rearrangement, as well as the internal thermo-oxidative degradation of the material due to the presence of air derived from the cellular structure. Peak B, which appeared as a shoulder, was related to the alcoholysis/hydrolysis decomposition. The very sharp peak named C was related to the thermo-oxidative degradation, similar to that explained for PC, though less intense as a result of less material remaining due to the previous degradation processes. Stage II, related to char oxidation [35], was observed at about the same temperature than in the case of PC. The shift towards higher values of the temperature corresponding to stage III was attributed to the porous developed char, which delayed heat transfer during its degradation. Once again, as for PC, no solid residues were obtained at the end of the thermo-oxidative decomposition.

3.1.2.2. Graphene nanoplatelets (GnP). The weight loss of graphene in air atmosphere was much more significant than under nitrogen, presenting a total loss of 89 wt% of its initial weight. Besides mass loss related to the removal of physically adsorbed water (around 100 °C), a three step weight loss was observed, with weight loss slope changes at 350, 500 and at 600 °C (see Fig. 7a). The decomposition of graphene in the presence of air was related to an acceleration of the degradation of functional groups that might remain from the fabrication, presumably due to pyrolysis of the labile oxygen-containing functional groups, yielding CO, CO_2 and

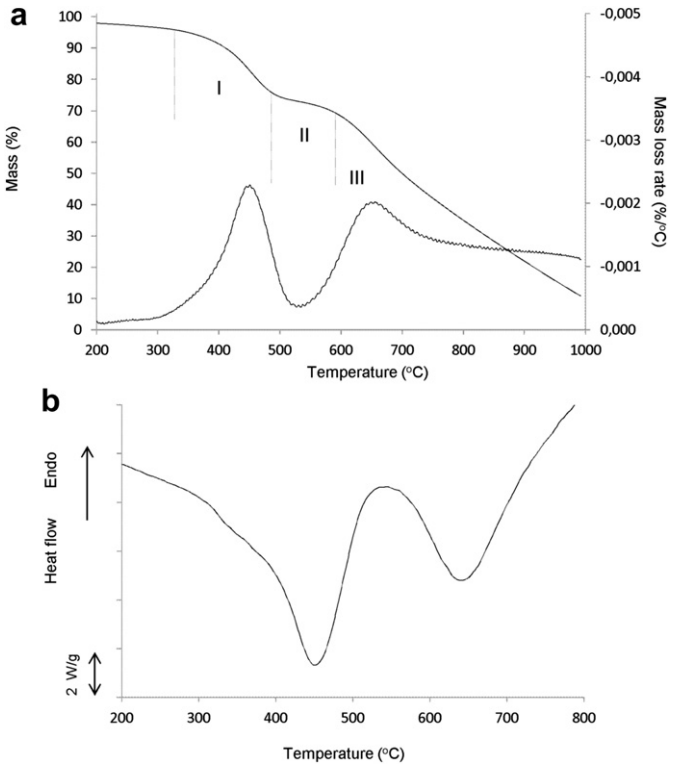

Fig. 7. (a) TGA and DTG thermograms and (b) heat flow curve under air atmosphere for the original graphene nanoplatelets (GnP), obtained at a heating rate of 10 °C/min.

H_2O [36]. The temperature corresponding to a 5 wt% loss was 351 °C, while for a 50 wt% loss it was 700 °C. The observed slope changes indicated that a vigorous degradation due to the presence of air was taking place, with the possibility of gas release accelerating the degradation of the material. Stage II illustrates the consumption of the protective char that formed during stage I. Stage III was related to the carbon oxidation of the material protected during the second stage, as well as the oxidation of the char that might have been simultaneously produced [31]. Two main exothermic processes can be observed in the heat flow curve of GnP presented in Fig. 7b, supporting the results of the TGA and DTG curves and showing that the first and third stages were clearly exothermic.

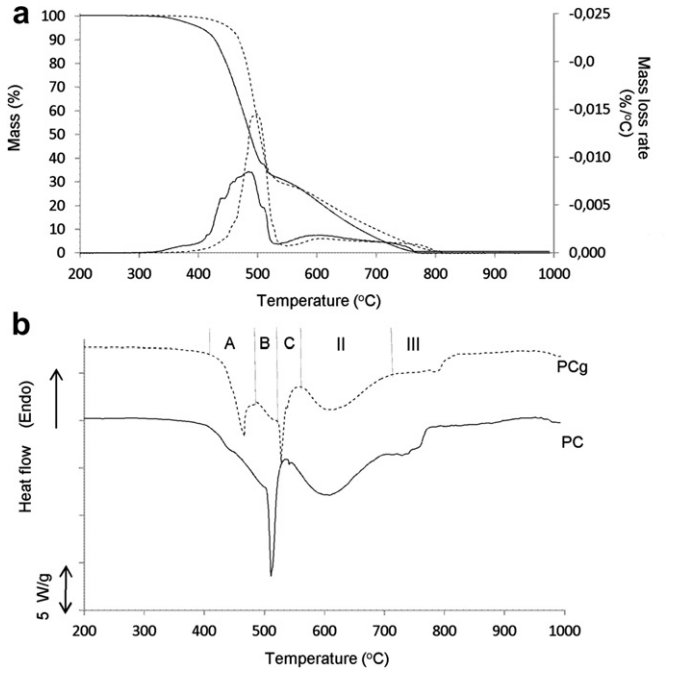

Fig. 8. (a) TGA and DTG thermograms and (b) heat flow curves under air atmosphere for the unfilled solid (PC, continuous line) and graphene-reinforced solid polycarbonate (PCg, dashed line), obtained at a heating rate of 10 °C/min.

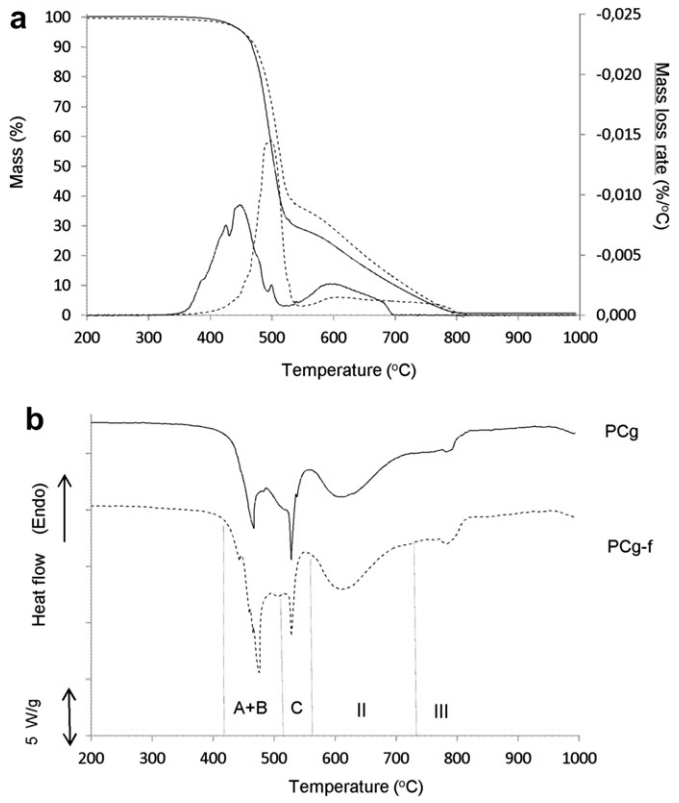

Fig. 9. (a) TGA and DTG thermograms and (b) heat flow curves under air atmosphere for the graphene-reinforced solid (PCg, continuous line) and graphene-reinforced foamed polycarbonate (PCg-f, relative density: 0.38, dashed line), obtained at a heating rate of 10 °C/min.

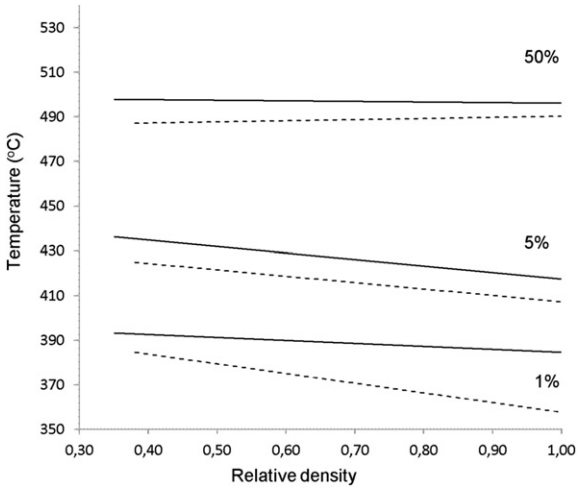

Fig. 10. Evolution of the decomposition temperature corresponding to 1, 5 and 50 wt% loss with relative density tested under air atmosphere (10 °C/min heating rate) for the unfilled (PC-f, dashed line) and graphene-reinforced foamed polycarbonate (PCg-f, continuous line).

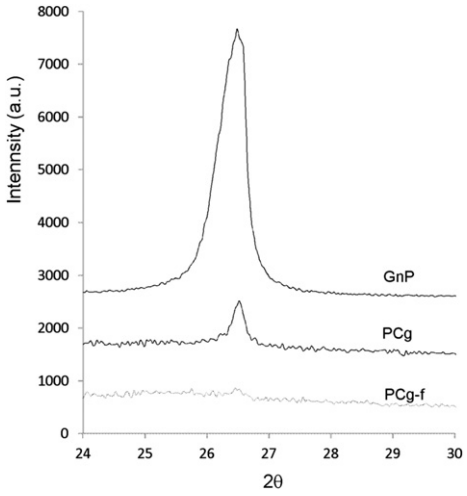

Fig. 11. X-ray diffraction patterns of GnP, PCg and PCg-f.

3.1.2.3. Graphene-reinforced polycarbonate. The graphene-reinforced solid polycarbonate (PCg), as can be seen in Fig. 8a, presented a three stage degradation, with a temperature at 1 wt% loss 30 °C higher than that of unfilled PC. Likewise, the temperatures for a 5 and 50 wt% losses were respectively 17 and 16 °C higher than for PC. Fig. 8a shows how the mass loss rates for PC and PCg were different due to the presence of graphene, its barrier effect delaying the escape of volatile gas products during degradation [33]. The DTG curve showed that T_{max} was 47 °C higher than for PC, this difference being smaller if compared to the respective values obtained in nitrogen. The heat flow curve presented in Fig. 8b showed an early but very sharp peak (peak A), attributed to the chain scission of the isopropylidene bonds and carbonate bonds undergoing rearrangement. Peak B corresponded to the alcoholysis/hydrolysis degradation processes. Last but not least, peak C was associated to the thermo-oxidative process, though in this case being considerably less intense than that of PC. This was related to a combination of an effective barrier effect of the graphene nanoplatelets, which made it harder for oxygen to reach the polymer, and less material remaining from the previous degradation processes. Stage II was related to the beginning of char oxidation [35] and was observed at about the same temperature as PC. Stage III almost disappeared and shifted up to higher temperatures, which was attributed to the tortuous path formed by the graphene nanoplatelets dispersed in the PC, resulting in a slower gas release. A small quantity of solid residue remained at 1000 °C, coinciding with the graphene content added to the materials.

The degradation for the graphene-reinforced foamed polycarbonate (PCg-f) was similar to the previously seen three stage degradation (Fig. 9a), presenting a slight delay on the degradation than that of the same material tested in nitrogen. The mass loss rate was very similar to that of PCg, presenting a slight difference that was attributed to the improved thermal insulating mechanism promoted by the cellular structure. The temperatures corresponding to the 1 and 5 wt% losses showed differences of 10 and 20 °C, respectively. On the other hand, the temperature at a 50 wt% loss was very similar between the unfoamed and foamed composites (see values presented in Table 2).

A similar thermal behaviour could be observed when analysing the heat flow curves presented in Fig. 9b, with the first peak (A + B) corresponding to the chain scission of the isopropylidene bonds and the alcoholysis and hydrolysis of the carbonate bonds. On the contrary, PCg presented two clearly defined peaks (peaks A and B), showing that these decomposition processes took place at different times.

PCg-f presented a sharp peak C in a similar manner and at about the same temperature as PCg. This was attributed to the formation of peroxides that underwent dissociation, caused by the presence of oxygen. These three peaks corresponded to stage I of the degradation, while stage II, which was observed at about the same temperature as the unfoamed compositae, was attributed to partial char oxidation [35]. Stage III presented a steeper slope than PCg, showing a similar exothermic behaviour with a slight increment in the area of the peak as seen in Fig. 9b, attributed to an improved exfoliation of graphene nanoplatelets during foaming, slightly reducing the barrier effect for the release of gases.

Fig. 10 presents the thermal degradation of the materials tested in air in terms of the relationship of the temperatures corresponding to 1, 5 and 50 wt% losses and relative density. A similar behaviour was found for the materials in terms of the 1 wt% loss temperatures when compared to the ones obtained in nitrogen. However, for both 5 and 50 wt% losses, the degradation temperatures for PC and PCg were very similar through a wide range of relative densities. It has to be noticed that the behaviour for the materials at 50 wt% loss was characterized by an almost horizontal line, indicating that the materials reached 50 wt% losses at similar temperatures. Generally speaking, the larger difference was observed during the beginning of the degradation, with lower temperatures being found than that obtained in nitrogen.

3.2. Dispersion of graphene nanoplatelets

The XRD patterns presented in Fig. 11 show how the graphene nanoplatelets, in their original form as supplied by the manufacturer (GnP), presented a strong sharp diffraction signal at $2\theta = 26.5°$

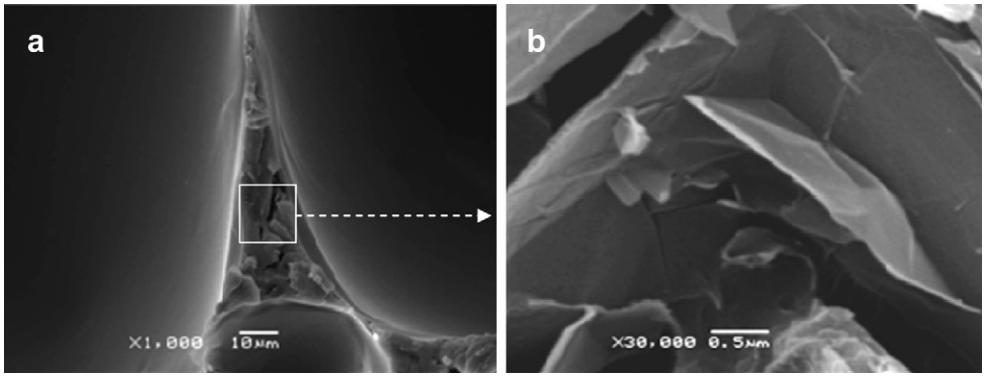

Fig. 12. (a) Cell strut present in the graphene-reinforced foamed polycarbonate (PCg-f) and (b) detail of dispersed graphene nanoplatelets in a cell strut.

characteristic of graphitic-like structures. The PCg showed the same peak, though with a lower intensity due to the lower concentration of graphene. Thus, no remarkable exfoliation could be achieved during melt-mixing. However, this peak almost disappeared for PCg-f, indicating the absence of layer-staking regularity, thus enabling to say that graphene nanoplatelets were partially exfoliated in thinner stacks or even in single graphene sheets [10,15]. Fig. 12a presents $a \times 1000$ magnified micrograph of one particular cell strut of the graphene-reinforced foamed polycarbonate. Fig. 12b shows a group of well-separated and clearly defined graphene nanoplatelets ($\times$30,000 magnification), enabling to get an idea of the thickness of the nanoplatelet stacks reached in the foamed composite.

4. Conclusions

The thermal decomposition of unfilled and graphene-reinforced solid and foamed polycarbonate was examined by thermogravimetry in both nitrogen and air atmospheres. It was found that the decomposition occurred in one step under nitrogen and in three steps in air. The thermal stability of PC was enhanced by foaming, with the lower relative density materials being the ones that delayed decomposition the most during the first stage in both atmospheres, related to a reduction of heat transfer due to the cellular structure. A linear relationship was found between the temperature of maximum mass loss and relative density. In addition, the well dispersed graphene nanoplatelets improved the thermal stability of polycarbonate due to their barrier effect, delaying the escape of volatile decomposition products during degradation. For the degradation in air, the graphene nanoplatelets also created a tortuous path for air, delaying the thermo-oxidative degradation of the material. Finally, a complete thermo-oxidative decomposition of the char formed in the first process was observed in air, accelerating the degradation and resulting in zero residues obtained at the end of the process.

The results presented in this work demonstrate that the combination of incorporating small amounts of graphene nanoplatelets to a polycarbonate matrix and later foaming significantly improve the thermal stability of polycarbonate, opening up a wider range of applications of this material as thermally-improved lightweight component.

Acknowledgements

The authors would like to acknowledge MICINN (Government of Spain) for the financial support of projects MAT2010-15565 and MAT2011-26410.

References

[1] Geim AK, Novoselov KS. The rise of graphene. Nat Mater 2007;6(3):183–91.
[2] Eda G, Chhowalla M. Graphene-based composite thin films for electronics. Nano Lett 2009;9:814–8.
[3] Potts J, Dreyer D, Bielawski C, Ruoff RS. Graphene-based polymer nanocomposites. Polymer 2011;52:5–25.
[4] Singh V, Joung D, Zhai L, Das S, Khondaker SI, Seal S. Graphene based materials: past, present and future. Prog Mater Sci 2011;56:1178–271.
[5] Salvagione HJ, Martinez G, Gomez MA. Synthesis of poly(vinyl alcohol)/reduced graphite oxide nanocomposites with improved thermal and electrical properties. J Mater Chem 2009;19:5027–32.
[6] Xu Z, Hong W, Bai H, Li C, Shi G. Strong and ductile poly(vinyl alcohol)/graphene oxide composite films with a layered structure. Carbon 2009;47:3538–43.
[7] Villar-Rodil S, Paredes JI, Martinez-Alonso A, Tascon JMD. Preparation of graphene dispersions and graphene-polymer composites in organic media. J Mater Chem 2009;19:3591–3.
[8] Liu N, Luo F, Wu H, Liu Y, Zhang C, Chen J. One-step ionic-liquid-assisted electromechanical synthesis of ionic-liquid-functionalized graphene sheets directly from graphite. Adv Funct Mater 2008;18:1518–25.
[9] Bhadra S, Khastagir D, Singh AK, Lee JH. Progress in preparation, processing and applications of polyaniline. Prog Polym Sci 2009;34:783–810.
[10] Song P, Cao Z, Cai Y, Zhao L, Fang Z, Fu S. Fabrication of exfoliated graphene-based polypropylene nanocomposites with enhanced mechanical and thermal properties. Polymer 2011;52(18):4001–10.
[11] Kim H, Macosko CW. Processing-property relationships of polycarbonate/graphene composites. Polymer 2009;50:3797–809.
[12] Kuilla T, Bhadra S, Yao D, Kim NH, Bose S, Lee J. Recent advances in graphene based polymer composites. Prog Polym Sci 2010;35:1350–75.
[13] Sengupta R, Bhattacharya M, Bandyopadhyay S, Bhowmick AK. A review on the mechanical and electrical properties of graphite and modified graphite reinforced polymer composites. Prog Polym Sci 2011;36(5):638–70.
[14] Stankovich S, Dikin DA, Dommett G, Kohlhaas KM, Zimney EJ, Stach E, et al. Graphene-based composite materials. Nature 2006;442:282–6.
[15] Liang JJ, Huang Y, Zhang L, Wang Y, Ma YF, Guo TY, et al. Molecular-Level dispersion of graphene into poly (vinyl alcohol) and effective Reinforcement of their nanocomposites. Adv Funct Mater 2009;19:2297–302.
[16] Rafiee MA, Rafiee J, Wang Z, Song HH, Yu ZZ, Koratkar N. Enhanced mechanical properties of nanocomposites at Low graphene content. ACS Nano 2009;3:3884–90.
[17] Zhao X, Zhang QH, Chen DJ. Enhanced mechanical properties of graphene based poly (vinyl alcohol) composites. Macromolecules 2010;43:2357–63.
[18] Xu L, Weiss RA. The effect of tosylate salts and zinc sulfonated polystyrene ionomer on the thermal stability of bisphenol A polycarbonate. Polym Degrad Stab 2004;84:295–304.
[19] Zhou W, Yang H. Flame retarding mechanism of polycarbonate containing methylphenyl-silicone. Thermochim Acta 2007;452:43–8.
[20] Hu Z, Chen L, Zhao B, Luo Y, Wang DY, Wang YZ. A novel efficient halogen-free flame retardant system for polycarbonate. Polym Degrad Stab 2011;96:320–7.
[21] Jang BN, Wilkie CA. TGA/FTIR and mass spectral study on the thermal degradation of bisphenol A polycarbonate. Polym Degrad Stab 2004;86:419–30.
[22] Jang BN, Wilkie CA. The thermal degradation of bisphenol A polycarbonate in air. Thermochim Acta 2005;426:73–84.
[23] Feng J, Hao J, Yang R. Flame retardancy and thermal properties of solid bisphenol A bis(diphenyl phosphate) combine with montmorillonite in polycarbonate. Polym Degrad Stab 2010;95:2041–8.
[24] Feng J, Hao J, Yang R. Using TGA/FTIR TGA/MS and cone calorimetry to understand thermal degradation and flame retardancy mechanism of polycarbonate filled with solid bisphenol A bis (diphenyl phosphate) and montmorillonite. Polym Degrad Stab 2012;97:605–14.
[25] Gibson RF. A review of recent research on mechanics of multifunctional composites materials and structures. Compos Struct 2010;92:2793–810.
[26] Antunes M, Mudarra M, Velasco JI. Broad-band electrical conductivity of carbon nanofibre-reinforced polypropylene foams. Carbon 2011;49:708–17.
[27] Verdejo R, Saiz-Arroyo C, Carretero-Gonzalez J, Barroso-Bujans F, Rodriguez-Perez M, Lopez-Manchado M. Physical properties of silicone foams filled with carbon nanotubes and functionalized graphene sheets. Eur Polym J 2008;44:2790–7.
[28] Yang J, Wu M, Chen F, Fei Z, Zhong M. Preparation, characterization, and supercritical carbon dioxide foaming of polystyrene/graphene oxide composites. J Superc Fluids 2011;56:201–7.
[29] Gedler G, Antunes M, Realinho V, Velasco JI. Novel polycarbonate-graphene nanocomposite foams prepared by CO_2 dissolution. IOP Conf Ser Mater Sci Eng 2012;31. Article ID 012008.
[30] Pham TA, Sik Kim J, Su Kim J, Jeong YT. One-step reduction of graphene oxide with L-glutathione. Colloids Surf A 2011;384:543–8.
[31] Wang G, Yang J, Park J, Gou X, Wang B, Liu H, et al. Facile Synthesis and characterization of graphene nanosheets. J Phys Chem C 2008;112(22):8192–5.
[32] Realinho V, Antunes M, Velasco JI, Haurie L. Fire behaviour of flame-retardant rigid polypropylene foams. Eurotec conference proceedings; 2011.
[33] Wang X, Yang H, Song L, Hu Y, Xing W, Lu H. Morphology, mechanical and thermal properties of graphene-reinforced poly(butylene succinate) nanocomposites. Compos Sci Technol 2011;72(1):1–6.
[34] Wang Y, Yi B, Wu B, Yang B, Liu Y. Thermal behaviors of flame-retardant polycarbonates containing SSK and PSPPP. J Appl Polym Sci 2003;89(4):882–9.
[35] Liu S, Ye H, Zhou Y, He J, Jiang Z, Zhao J, et al. Study on flame-retardant mechanism of polycarbonate containing sulfonate-silisesquioxane-fluoro retardants by TGA and FTIR. Polym Degrad Stab 2006;91:1808–14.
[36] Stankovich S, Dikin D, Piner R, Kohlhaas K, Kleinhammes A, Jia Y, et al. Synthesis of graphene-based nanosheets via chemical reduction of exfoliated graphite oxide. Carbon 2007;45:1558–65.